



TM-1019  
1183.000

p(42)Be NEUTRON THERAPY BEAMS:  
DOSE RATE AND PENETRATION AS A FUNCTION OF  
TARGET THICKNESS AND BEAM FILTRATION

I. Rosenberg and M. Awschalom

Fermilab, P. O. Box 500, Batavia, Illinois 60510, USA

T. Y. Kuo and J. L. Tom

The Cyclotron Corporation, Berkeley, California 94710, USA

December 1980

p(42)Be NEUTRON THERAPY BEAMS:

DOSE RATE AND PENETRATION AS A FUNCTION OF  
TARGET THICKNESS AND BEAM FILTRATION.

ABSTRACT

It is shown that, in the production of p(42)Be neutron beams for clinical use, the use of semi-thick targets leads to more desirable beam characteristics, when appropriate backstop materials are used.

Furthermore, an algebraic representation of beam penetration and of dose per unit charge on target, including hardening by polyethylene filters, provides a method for target optimization.

Key words: neutron, target, optimization, clinical, power, depth-dose

## INTRODUCTION

In a previous paper<sup>1</sup>, it was argued that an improvement in beam quality and dose rate at constant target power dissipation for a (p,Be) neutron therapy beam could be achieved by making the target thinner than the proton range and by absorbing the excess proton energy in a material with good thermal properties and small neutron production cross-section. This design would reduce the contribution to the neutron flux from lower energy inelastic reactions, thus improving the clinical quality of the neutron beam. Moreover, the high energy density deposited at the Bragg peak region would take place away from the beryllium disk. This would allow larger current densities on target and lead to correspondingly larger dose rates.

The results of an experiment carried out to test this concept have been previously reported<sup>2</sup>. Those results were obtained using a rather thick (2 mm) copper backstop and were inconclusive for the thinner targets. It was then hypothesized that the thick copper proton backstop contributed a significant flux of low penetration neutrons to that produced in the thinner Be-targets, thus masking the changes due to the thinning of the targets. Therefore, a new target assembly was designed with a more favorable proton beam stop. This consisted of the cooling water and a

pyrolytic graphite proton stop. The measurements were repeated at the Cyclotron Corporation<sup>3</sup>.

#### EXPERIMENTAL ARRANGEMENTS

The same CP42 cyclotron was used as in the previous experiment.<sup>2</sup> An isocentric gantry had been added to the beam line and shielding had been added around the target assembly. The proton energy was measured as being  $41.3 \pm 0.2$  MeV by the range-energy method. The target assembly included a vacuum barrier consisting of a 0.25 mm thick copper sheet on which the Be targets were brazed, followed downstream by a 1.3 mm layer of flowing cooling water, a 8.0 mm pyrolytic graphite backstop, and 2.6 mm of stainless steel. Even excluding the stainless steel, this was enough to stop protons emerging from the thinnest Be-target used. Dual transmission chambers, made of aluminum, and a filter holder were located downstream of the target assembly. The beam hardening polyethylene filters were placed between the target and the upstream end of the collimator. The gantry was rotated so that a horizontal beam could be projected onto the same tissue equivalent liquid phantom already described<sup>2</sup>. The density of the liquid was  $1.071 \pm 0.005$  g cm<sup>-3</sup>. The 10x10 cm<sup>2</sup> collimator and a source-to-surface distance of

125 cm were used for all measurements.<sup>2</sup> All data were taken using a single ionization chamber, and the phantom-chamber set-up was never disturbed throughout the changes of targets and filters. The chamber used was a 0.1 cc, EG&G model IC-18, A-150 plastic thimble chamber of outside diameter 0.8 cm and 0.16 cm wall thickness<sup>4</sup>. The position and travel of the chamber along the central axis of the beam were checked with a transit, and its depth in the phantom was calibrated using a stainless steel gauge bar. Measurements were taken for each target configuration in the region of maximum dose until its value was established, and at several depths bracketing the position of half-maximum dose. This latter depth was then derived by interpolation. All depths are defined at the center of the chamber. They include the 0.125 mm thick front window of the Lucite tank. All other experimental arrangements were similar to those described in the previous paper.<sup>2</sup>

## RESULTS

In all, four target thicknesses were used for this investigation. These thicknesses corresponded closely to those previously reported<sup>2</sup>:

"A" pure beryllium target, 1.21 cm thick, density  $1.84 \text{ g cm}^{-3}$ , which would stop 41.3 MeV protons completely;

"B" HP-20 target, 0.80 cm thick, which would remove 22.8 MeV from a 41.3 MeV proton beam.

"C" HP-20 target, 0.59 cm thick, which would remove 15.4 MeV from a 41.3 MeV proton beam;

"D" HP-20 target, 0.34 cm thick, which would remove 8.2 MeV from a 41.3 MeV proton beam.

The HP-20 Type I material is sintered Be containing 99.30% elemental Be, 0.66% elemental oxygen, .04% being C, Fe, Al, Mg, and Si, by weight.<sup>5</sup> These samples had a density of  $1.85 \text{ g cm}^{-3}$ .

All targets were investigated with no filtration, and also with 3 cm ( $2.9 \text{ g cm}^{-2}$ ) and 5 cm ( $4.8 \text{ g cm}^{-2}$ ) thick unborated polyethylene filters in the neutron beam upstream from the collimator. Although the measurements did not provide values of absolute dose per unit charge, the stability of the equipment allowed precise dose rate ratios to be obtained.

A summary of the results is presented in Table 1. The observed fluctuations in the values of ionization chamber charge collected per unit charge on target, as well as temperature and pressure, lead to a  $\pm 1\%$  uncertainty in the values of relative dose rates. This translates to  $\pm 1$  mm uncertainty in the interpolated values of the depth for half-maximum dose. To this uncertainty, the following uncertainties must be added in quadrature:

1. scatter in the points for interpolation ( $\pm 1.0\%$ ),
2. errors in the reproducibility of the chamber depth ( $\pm 1.0$  mm), and
3. uncertainties in the displacement correction factor<sup>6</sup>,

for a total uncertainty of  $\pm 2$  mm in the value of the depth for half-maximum dose.

Fig. 1 shows the dose per unit charge at the depth of maximum dose for all target and filter configurations normalized to the dose per unit charge from the unfiltered thick "A" target. The symbols are as large as the uncertainties. The two dashed lines represent predictions

for unfiltered thin target yields, given by the empirical relation<sup>1</sup>:

$$\frac{D(e_t, 0)}{D(E_i, 0)} = 1 - \left( \frac{E_i - e_t}{E_i} \right)^\beta \quad (1)$$

where  $D(e_t, 0)$  is the dose rate at  $D_{\max}$  per unit proton current from an unfiltered target of such thickness that it absorbs by ionization an energy  $e_t$  from protons having an incident energy  $E_i$ .<sup>1</sup>  $D(E_i, 0)$  thus corresponds to an unfiltered beam-stopping (thick) Be-target. Values for  $\beta$  of 2.8<sup>7,8</sup> and 3.2<sup>1</sup> are shown; the former agrees well with the results of targets "B" and "C", the latter with the results of target "D" only. A choice for  $\beta$  of 2.8 was made from these results, since the value for target "D" may be affected by some neutron production in the graphite, where the threshold for the (p,n) reaction is about 20 MeV.<sup>9</sup>

Fig. 2 shows the variation of the depth for half-maximum dose with target thickness and filtration. The depths are expressed in cm of TE liquid (1 cm = 1.07 g cm<sup>-2</sup>), for an SSD of 125 cm and a field size, defined at  $d_{\max}$  for the 50% decrement lines, of 10x10 cm<sup>2</sup>. The dashed line joining the unfiltered target points represent an empirical relationship given by the expression:

$$\frac{Z(e_t, 0)}{Z(E_i, 0)} = 1 + a \left( \frac{E_i - e_t}{E_i} \right)^b \quad (2)$$

where  $Z(e_t, 0)$  and  $Z(E_i, 0)$  are the depths for half-maximum dose corresponding to target thicknesses of  $e_t$  and  $E_i$ , respectively.

The constants  $a$  and  $b$  have been calculated by a least square fit of the unfiltered target data. They are:

$a = 0.18$  and  $b = 1.40$  for the lowest curve shown in Fig.

2.

The curves joining the filtered target points have been obtained in a similar way.

The use of the thinner Be-targets will cause an increase in the activation of the target cooling water. If the residual energy of the protons exiting the thinner targets is high enough, various radionuclides can be produced in the water through reactions such as  $^{16}\text{O}(p, p'n)^{15}\text{O}$ ,  $^{16}\text{O}(p, p'2n)^{14}\text{O}$ ,  $^{16}\text{O}(p, \alpha)^{13}\text{N}$  and  $^{16}\text{O}(p, p'\alpha n)^{11}\text{C}$ . These radioactive products can then be carried by the water flow around the closed cooling loop. During residual radiation build-up measurements, it was indeed noticed that the exposure rate from the water lines increased significantly while using the thinnest ("D") target. However, no quantitative measurements of this effect were made during this experiment.

Preliminary exposure rate build-up measurements were made at various locations around the treatment head, during a cycle of four irradiations of 100 rad to  $D_{max}$  every hour for three hours, for various target-filter combinations having comparable penetration ( A5, C3 and D0 in Fig. 3). Within the precision of the measurements (of the order of 50%), no significant difference in remanent radioactivity between these target configurations could be detected 5 minutes after each irradiation.

DISCUSSION OF RESULTS

The present results closely support earlier predictions<sup>1</sup>, and further show the effect of different backstop materials when thinner targets are used<sup>2</sup>. It can be seen from Table 1 and Fig. 2 that there is a monotonic improvement in penetration as the targets are made thinner. Furthermore, the beam attenuation by the filters decreases with thinner targets, indicating a harder unfiltered beam. The improvement in penetration due to the filters, for any given target thickness, is directly related to the filter's attenuation. This can be expressed by an empirical relation:

$$\frac{Z(e_t, \text{filt})}{Z(e_t, 0)} = 1 + m \left[ 1 - \frac{D(e_t, \text{filt})}{D(e_t, 0)} \right] \quad (3)$$

where  $Z(e_t, \text{filt})$  and  $D(e_t, \text{filt})$  refer to the depth for half-maximum dose and the maximum dose rate per unit current, respectively, from the filtered targets, and  $Z(e_t, 0)$  and  $D(e_t, 0)$  correspond to the same target but without filtration. A fixed value for  $m$  of 0.25 was derived by least square fits to the available data, since there was no discernible trend with target thickness.

Comparison of the present results with those reported previously using a thick copper backstop<sup>2</sup> shows, as expected, that the effects of the choice of backstop material show up only for the thinner targets.

There is good agreement in the penetration and relative dose rate values from both experiments for targets "A" and "B", and also for target "C" with heavy filtration. The significant divergences occur in the penetration results for the unfiltered "C" target and more markedly for target "D".

In fact, there should be no backstop effect for the thick target "A", and the agreement between the two results for this target is a measure of the reliability of the measurements. These results also agree rather well with recent measurements of a  $p(45)\text{Be}(45)$  neutron beam<sup>10</sup>, after appropriate corrections are made for beam energy, SSD, and the use of water instead of TE-solution in the phantom. The relative dose rate per unit proton current from the unfiltered target "D" still seems to be higher than that

predicted by extrapolation from the other targets (Fig. 1). This effect is probably due to neutron production in the graphite backstop by protons of energy well in excess of the 20 MeV threshold. These lower energy neutrons would tend to reduce the effect of thinning the target.

The experimental set-up had not been designed to measure the build-up region. However, there were indications while searching for the depth of maximum dose that the location of the maximum may be deeper, and that the approach to maximum from the surface may be more gradual, for the thinner targets. Proper measurements with an extrapolation chamber are called for to confirm this impression.

#### TARGET DESIGN

When designing a target for a (p,Be) therapy neutron beam a compromise among several characteristics of the beam must be sought. The most important requirements are to maximize the treatment dose rate, the depth for half-maximum dose, and the skin sparing obtainable with the available proton energy and current, all within allowable power densities in the target. To illustrate this point, the results presented in Table 1 and in Figs 1 and 2 have been replotted in Fig. 3. Here, the maximum dose per unit proton

charge on target from all measured target configurations, normalized to the unfiltered thick "A" target dose, has been plotted against the corresponding depth for half-maximum dose. The first two above criteria require that a configuration closest to the upper right-hand corner of the graph be chosen. Trade-offs are involved both in making the target thinner and in filtering its output. In fact, by combining eq. 1 and 2, an empirical relation can be derived between the two plotted parameters for the unfiltered targets:

$$\frac{D(e_t, 0)}{D(E_i, 0)} = 1 - \left[ \frac{1}{a} \left( \frac{Z(e_t, 0)}{Z(E_i, 0)} - 1 \right) \right]^{\beta/b} \quad (4)$$

where all terms have been defined before.

The continuous curve shown in Fig. 3 represents this relationship with the values for a, b and  $\beta$  derived above. Also shown in Fig. 3, with dashed lines, are the relationship of filtered to unfiltered targets as expressed in equation 3. These curves agree well with the data. It is evident that the optimum target thickness to maximize the first two above criteria should be the one corresponding to the point on the target-effect curve (Eq. 4) at which the slope equals that of the filter-effect curve (Eq. 3). Any further improvement in penetration achieved by filtration from this point will be at a higher dose rate per unit proton

current than achievable with any other target/filter combination. In fact, target "B" is fortuitously close to this optimum.

However, another factor has to be kept in mind. The activation of the target area and of the head shielding, as well as the leakage radiation from the head, should be kept to a minimum. The use of a hardening filter reduces the useful dose to the patient for the same total number of neutrons produced in the target. Therefore, for a given dose delivered to the patient, a thinner filter should produce a lower level of activation. Thus, if there were a choice of different target/filter combinations giving the same penetration, a configuration requiring less filtration should be preferred to minimize this activation, especially from long-lived radionuclides. For short-lived activity, the preliminary measurements mentioned above seem to indicate that the difference between various target/filter combinations is small. Fortunately, the target-effect curve (Eq. 4) drops slowly close to the above optimum region, and only a small loss in dose per unit proton charge is suffered by selecting a thinner target and a thinner filter to achieve the same penetration as from the optimum target/filter combination. Furthermore, the thinner target could allow the use of a higher proton beam current within the same power density limitations<sup>1</sup>. Thus, if the accelerator is capable of

higher currents, an equal or higher treatment dose rate could be achieved. In fact, target "C" seems, also fortuitously, to come close to fitting this criterion.

### CONCLUSIONS

The present results for a p(42)Be neutron beam, obtained using a target much better shielded than in the previous experiment<sup>2</sup> and a carefully designed backstop, support the predictions of the original target design concept<sup>1</sup>, namely, that the use of semi-thick Be-targets can improve the performance of clinical neutron generators using energetic proton beams. Higher penetrations are achievable using thinner targets, for a relatively small loss in dose rate per unit proton current, and potentially higher treatment dose rates, compared to thick targets.

The choice of proton backstop material can influence the penetration if the target is made very thin. Residual proton energies above the (p,n) threshold for the chosen backstop material will produce low energy neutrons that will tend to limit the improvement in beam quality due to the thinning of the Be-target.

A graphical method has been presented for selecting the optimum combination of target and filter thicknesses based on the above performance criteria. While the empirical relations obtained here are only valid for an incident energy of 41.3 MeV, similar experiments should be carried out on dedicated neutron therapy generators operating at other proton energies.

ACKNOWLEDGEMENTS

The authors gratefully acknowledge G.O.Hendry for his numerous suggestions and valuable comments throughout this program and F.A.Ramsey and his staff for their assistance with the operation of the cyclotron during these measurements.

This work was supported in part with funds from NCI Grant No.5P01CA18081 and the Cyclotron Corporation.

REFERENCES

1. Miguel Awschalom, Ivan Rosenberg, "Conceptual Design Beryllium Targets for the Generation of Neutron Beams for Radiation Therapy by the (p,n) Reaction," Med.Phys. 7, 492 (1980).
2. Miguel Awschalom, Ivan Rosenberg, T. Y. Kuo, J. L. Tom, "The Influence of Target Thickness and Backstop Material on Proton-Produced Neutron Beams for Radiotherapy," Med.Phys. 7, 495 (1980).
3. The Cyclotron Corporation, 950 Gillman Street, Berkeley, Ca. 94710, USA.
4. EG&G ionization chambers are now made by Far West Technology, Goleta, Ca. 93017, USA.
5. Kaweki Berylco Industries, Inc., Hazleton, Pa. 18201, USA.
6. P.Shapiro, F.H.Attix, L.S.August, R.B.Theus, "Displacement Correction Factor for Fast Neutron Dosimetry in Tissue Equivalent Phantom," Med.Phys. 3, 87 (1976).

7. W.M.Quam, S.W.Johnson, G.O.Hendry, J.L.Tom, P.H.Heintz, R.B.Theus, "Dosimetry Measurements of 26, 35 and 45 MeV p-Be and p-Li Neutron Beams," Phys.Med.Biol. 23, 47 (1978).
  
8. F.M.Waterman, F.T.Kuchnir, L.S.Skaggs, R.T.Kouzes, W.H.Moore, "Neutron Spectra from 35 and 46 MeV Protons, 16 and 28 MeV Deuterons and 44 MeV <sup>3</sup>He-Ions on Thick Beryllium," Med.Phys. 6, 432 (1979)
  
9. R.J.Howerton, D.Braff, W.J.Cahill, N.Chazan, Thresholds of Nuclear Reactions, UCRL-14000, May, 1964.
  
10. D.K.Bewley, J-P.Meulders, M.Octave-Prignot and B.C.Page, Phys.Med.Biol. 25, 887 (1980).

TABLE CAPTIONS

TABLE 1

p(42)Be( $e_t$ ) NEUTRON BEAM:

DOSE RATE AND PENETRATION AS A FUNCTION OF  
TARGET THICKNESS AND BEAM FILTRATION.

## Foot Notes:

1. Number in parenthesis is the fraction of incident proton energy lost in the target by ionization.
2. Relative dose at  $D_{max}$  per unit proton charge on target, normalized to one hundred for the unfiltered thick target "A". The standard deviation includes 0.3% uncertainty for temperature and pressure correction over the whole period of the experiment.
3. Relative dose at  $D_{max}$  per unit proton charge on target, normalized to one hundred for the unfiltered output from each target. The standard deviation includes 0.1% uncertainty for temperature and

pressure correction over each target measurement period.

4. Depth for  $D_{\max}/2$ . The standard deviation for these values is estimated to be 0.2 cm.
5. Relative improvement in the depth for  $D_{\max}/2$  obtained with filtration for each target.

TABLE 1

TARGET		FILTER	Rel. Dose Unit Charge	Rel. Dose Unit Charge	$Z_{D_{max}/2}$ cm	$\frac{z(\text{filt})}{Z(0)}$
ID	$\Delta E$ (MeV)	Thick- ness				
A	41.3	0	100.0	100.0	11.5	1.000
A	(1.000)	3 cm	73.1 $\pm$ 0.5	73.1 $\pm$ 0.4	12.3	1.070
A		5 cm	62.1 $\pm$ 0.5	62.1 $\pm$ 0.4	12.6	1.096
B	22.8	0	88.0 $\pm$ 0.5	100.0	12.2	1.000
B	(0.522)	3 cm	66.3 $\pm$ 0.5	75. $\pm$ 0.2	12.9	1.057
B		5 cm	56.7 $\pm$ 0.5	64.5 $\pm$ 0.2	13.2	1.082
C	15.4	0	73.4 $\pm$ 0.4	100.0	12.6	1.000
C	(0.373)	3 cm	56.3 $\pm$ 0.5	76.7 $\pm$ 0.2	13.4	1.063
C		5 cm	48.8 $\pm$ 0.4	66.5 $\pm$ 0.1	13.5	1.071
D	8.2	0	49.8 $\pm$ 0.4	100.0	13.1	1.000
D	(0.198)	3 cm	38.4 $\pm$ 0.4	77.1 $\pm$ 0.1	13.7	1.046
D		5 cm	33.8 $\pm$ 0.4	67.9 $\pm$ 0.1	14.2	1.084
Notes: 1			2	3	4	5

FIGURE CAPTIONS

Fig. 1. Relative dose at  $D_{\max}$  per unit charge (D), normalized to unity for the unfiltered "A" target, for various target/filter configurations. The curves joining the unfiltered targets points correspond to the empirical relation:

$$\frac{D(e_t, 0)}{D(E_i, 0)} = 1 - \left( \frac{E_i - e_t}{E_i} \right)^\beta$$

for values of  $\beta$  shown in the Figure.

Fig. 2. Depth of half-maximum dose (Z), for various target/filter configurations. The dashed curve joining the unfiltered targets points corresponds to the empirical relation:

$$\frac{Z(e_t, 0)}{Z(E_i, 0)} = 1 + 0.18 \left( \frac{E_i - e_t}{E_i} \right)^{1.4}$$

Fig. 3. Relative dose at  $D_{\max}$  per unit charge (D), normalized to unity for the unfiltered "A" target, for various targets and hardening filters, versus half-maximum depth (Z). Labels "Xn" near the symbols identify target "X" with filter thickness "n" cm. Dashed lines connect points for the same target according to the empirical relation:

$$\frac{Z(e_t, \text{filt})}{Z(e_t, 0)} = 1 + 0.25 \left[ 1 - \frac{D(e_t, \text{filt})}{D(e_t, 0)} \right]$$

The solid line corresponds to the empirical relation for unfiltered targets:

$$\frac{D(e_t, 0)}{D(E_i, 0)} = 1 - 30.9 \left[ \frac{Z(e_t, 0)}{Z(E_i, 0)} - 1 \right]^{2.0}$$

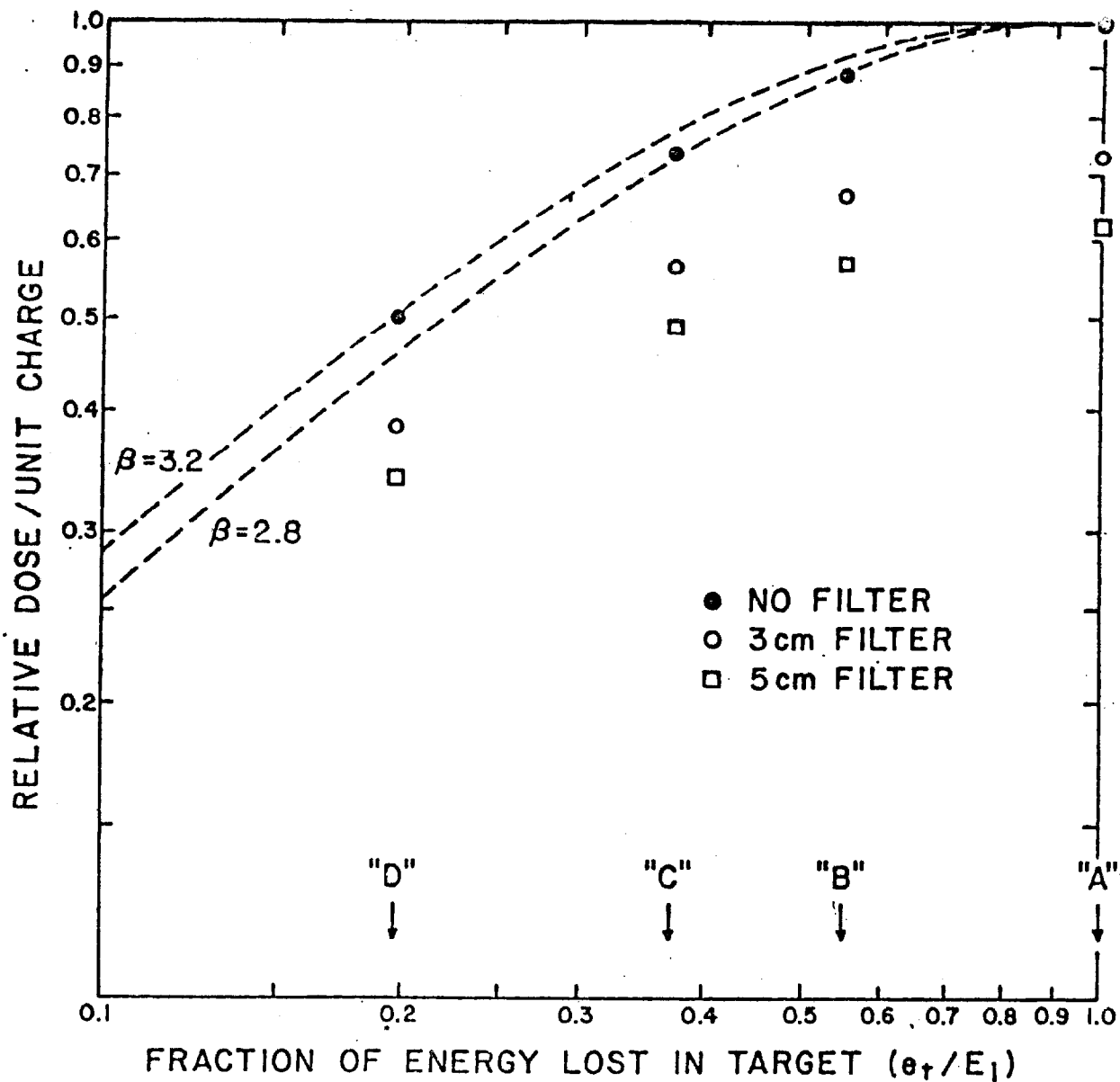


Figure 1

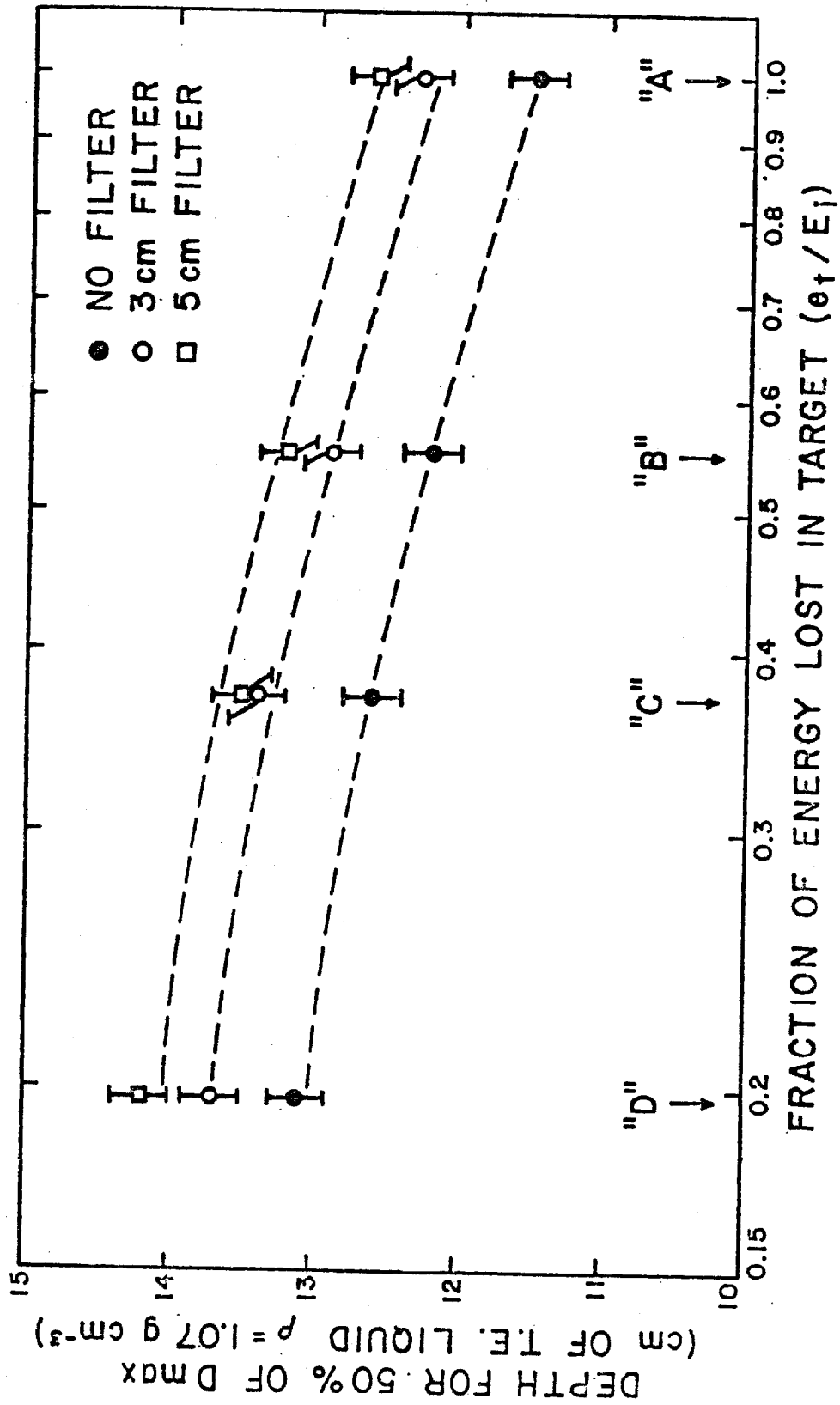


Figure 2

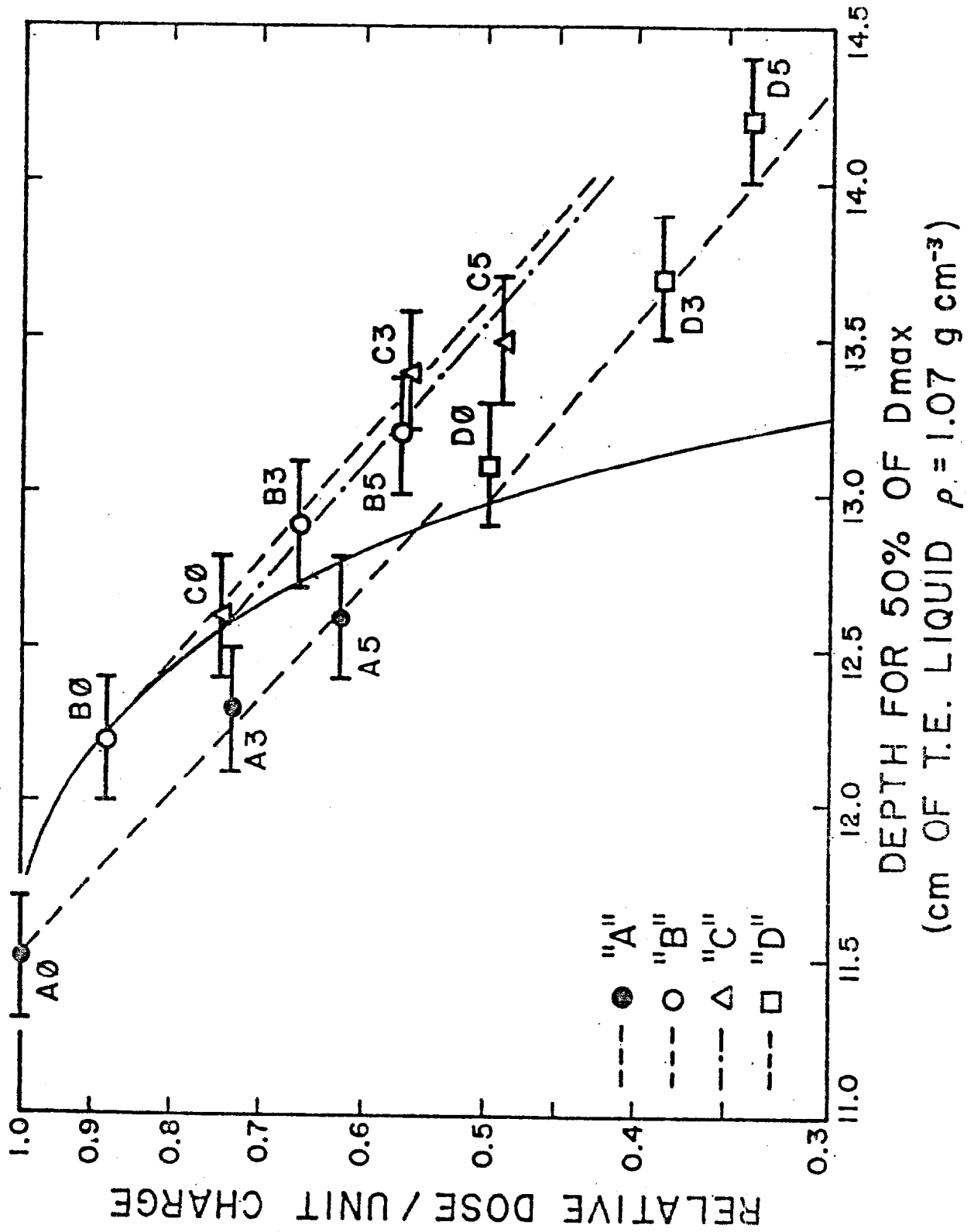


Figure 3